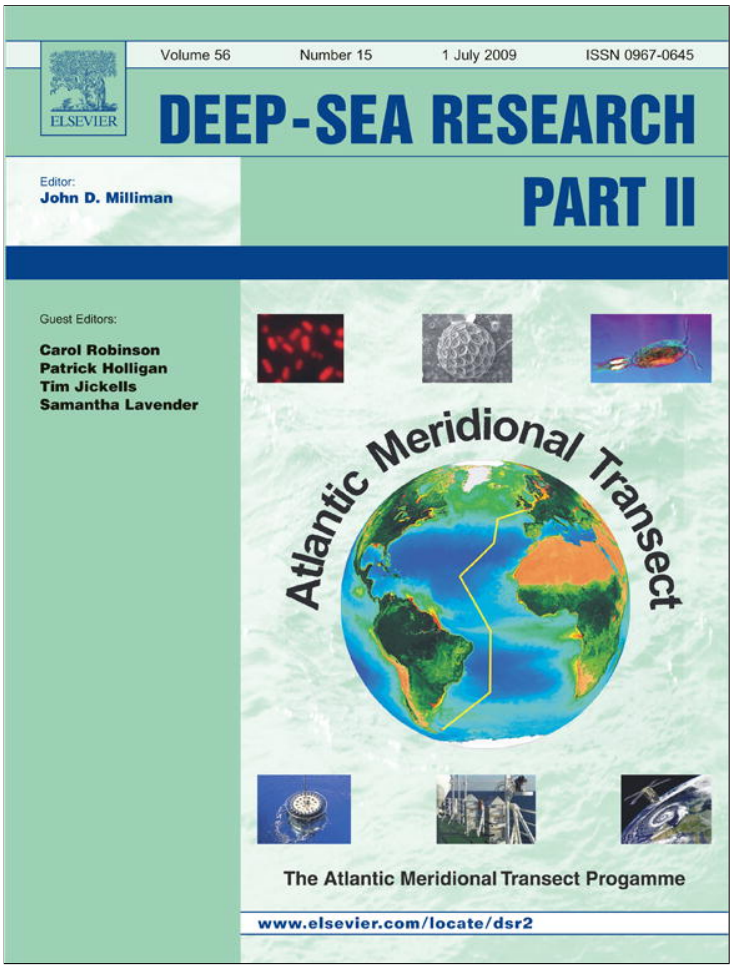

Deep-Sea Research II 56 (2009) 931–940

Contents lists available at ScienceDirect

Deep-Sea Research II

journal homepage: www.elsevier.com/locate/dsr2

Seasonal and spatial variability in plankton production and respiration in the Subtropical Gyres of the Atlantic Ocean

Niki Gist [a], Pablo Serret [b], E.M.S. Woodward [a], Katie Chamberlain [a], Carol Robinson [a,*,1]

[a] Plymouth Marine Laboratory, Prospect Place, Plymouth PL1 3DH, UK
[b] Departamento de Ecología y Biología Animal, Universidad de Vigo, 36200 Vigo, Spain

ARTICLE INFO

Article history:
Accepted 1 October 2008
Available online 27 November 2008

Keywords:
Plankton
Production
Respiration
Atlantic Ocean
Gyres
Atlantic Meridional Transect

ABSTRACT

Euphotic zone plankton production (P) and respiration (R) were determined from the *in vitro* flux of dissolved oxygen during six latitudinal transects of the Atlantic Ocean, as part of the Atlantic Meridional Transect (AMT) programme. The transects traversed the North and South Atlantic Subtropical Gyres (N gyre, 18–38°N; S gyre, 11–35°S) in April–June and September–November 2003–2005. The route and timing of the cruises enabled the assessment of the seasonal variability of P, R and P/R in the N and S gyres, and the comparison of the previously unsampled N gyre centre with the more frequently sampled eastern edge of the gyre. Mean euphotic zone integrated rates ($\pm$SE) were $P=63\pm23$ ($n=31$), $R=69\pm22$ ($n=30$) mmol O_2 m^{-2} d^{-1} in the N gyre; and $P=58\pm26$ ($n=30$), $R=62\pm24$ ($n=30$) mmol O_2 m^{-2} d^{-1} in the S gyre. Overall, the N gyre was heterotrophic ($R>P$) and it was more heterotrophic than the S gyre, but the metabolic balance of both gyres changed with season. Both gyres were net heterotrophic in autumn, and balanced in spring. This seasonal contrast was most pronounced for the S gyre, because it was more autotrophic than the N gyre during spring. This may have arisen from differences in nitrate availability, because spring sampling in the S gyre coincided with periods of deep mixing to the nitracline, more frequently than spring sampling within the N gyre. Our results indicate that the N gyre is less heterotrophic than previous estimates suggested, and that there is an apparent decrease in R from the eastern edge to the centre of the N gyre, possibly indicative of an allochthonous organic carbon source to the east of the gyre.

1. Introduction

The magnitude of plankton production (P) and respiration (R) are crucial to our understanding of the biogeochemistry of the oceans, since the balance between them indicates the amount of biologically fixed carbon available for export to the deep ocean, or for return to the atmosphere. The oligotrophic gyres are of prime importance to our understanding of how atmospheric CO_2 is influenced by the ocean carbon cycle (Neuer et al., 2002). They cover more than 60% of the global ocean, make a significant contribution to global productivity (Marañón et al., 2003; McClain et al., 2004), and export up to 50% of global carbon (Emerson et al., 1997). However, the P/R balance of these vast regions has not been satisfactorily determined. There is a lack of open ocean P and R data, with respiration measurements being particularly sparse (Robinson and Williams, 2005).

Analysis of the limited P and R data that do exist, has led to differing conclusions. Serret et al. (2002) attributed observations of a net heterotrophic ($P<R$) N gyre coincident with a more balanced S gyre to biogeochemical differences in gyre functioning. However, although net heterotrophy has been consistently observed in the subtropical N Atlantic (Duarte et al., 2001; Serret et al., 2001, 2002; Moran et al., 2004), one Atlantic Ocean latitudinal study suggested that the S gyre is more heterotrophic than the N gyre (González et al., 2002). The gyres are not homogeneous, static systems (Marañón et al., 2003; McClain et al., 2004), and these different interpretations may simply be due to different temporal and spatial ranges in the data collected by Serret et al. (2002) and González et al. (2002). The determination of how P and R vary temporally and spatially within the gyres therefore remains an essential prerequisite to accurately assess the level of autotrophy ($P>R$) to heterotrophy, and so the implied biological source or sink of CO_2 from the ocean to the atmosphere.

Using measurements collected east of 32°W in the N Atlantic, Duarte et al. (2001) estimated the carbon source required for the measured net heterotrophy to be as high as 0.5 Pg C yr^{-1} for the North Atlantic subtropical gyre-east (NAST-E; Longhurst, 1998). This dataset could not confirm whether the observed imbalances

* Corresponding author. Tel.: +44 1603 593174; fax: +44 1603 591327.
E-mail address: Carol.Robinson@uea.ac.uk (C. Robinson).
[1] Present address: School of Environmental Sciences, University of East Anglia, Norwich NR4 7TJ, UK.

0967-0645/$ - see front matter © 2008 Elsevier Ltd. All rights reserved.
doi:10.1016/j.dsr2.2008.10.035

extended throughout the gyre, or if they were only characteristic of the northeastern region. The analysis of spatial variability is also pertinent within the N gyre because net heterotrophy in the region may be supported by allochthonous carbon sources originating, for example, in the northwest African upwelling, or from atmospheric inputs of organic matter (Robinson et al., 2002; Pelegri et al., 2005; Duarte et al., 2006; Serret et al., 2006), which might lead to a gradient in *R* from the eastern edge to the centre of the gyre (Serret et al., 2006). Certainly, previous estimates of net heterotrophy within the N gyre were too high to be supported by local, simultaneously produced carbon (Duarte et al., 2001; Serret et al., 2002). Both *P*/*R* and primary production (PP) exhibit pronounced seasonal variability (González et al., 2002; Marañón et al., 2003; Teira et al., 2005), and the accumulation of carbon produced during the more productive seasons may lead to the decoupling of *P* and *R* over large spatial or temporal scales (Serret et al., 2001). Inter-annual measurements are also important, as they allow the assessment of both natural temporal variability and long-term trends (Karl et al., 2001). This is particularly important in the context of recent evidence which indicates that the gyres are expanding (McClain et al., 2004), as well as the suggestion that future climate warming could lead to increases in stratification and the geographical extent of the gyres within the oceans (Sarmiento et al., 2004).

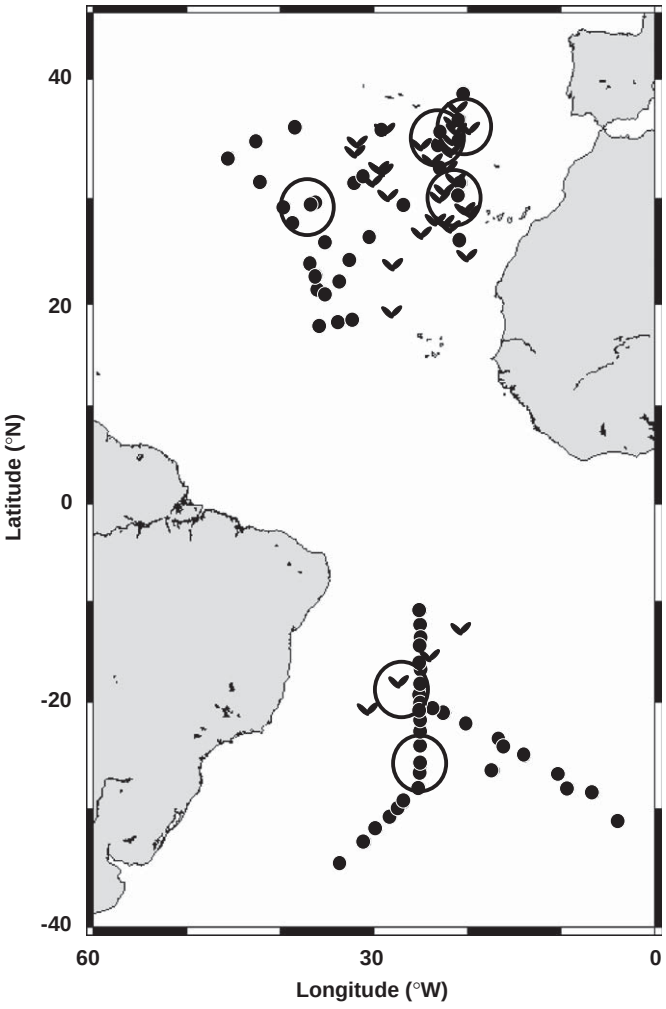

Fig. 1. Locations of the rate measurements considered in our analysis from AMT 12–17 (circles) and from previously published studies (crescents) obtained from www.amt-uk.org/data/respiration.xls. Regions indicated by the large open circles are the approximate positions of the SeaWiFS data given in Fig. 5.

Since 1995, the Atlantic Meridional Transect programme (AMT; www.amt-uk.org) has undertaken biological, chemical and physical oceanographic research during the annual return passage of research vessels between the UK and the South Atlantic. The programme aims to study ocean plankton ecology and biogeochemistry, and their interaction with atmospheric processes. The present study took place during six latitudinal transects, AMT 12–17, in the years 2003–2005. The cruise transects traversed a range of ecosystems, but in the present study we will only consider the N and S Atlantic gyres. Prior to this study, *P*/*R* had not been measured in the N gyre any further west than 32°W, and only two studies had measured *P* and *R* in the S gyre (González et al., 2002; Serret et al., 2002). The bi-annual sampling regime in both gyres enabled the direct comparison of the gyres at the same time of the year (during opposite seasons), and also within the same season (at different times of year). Cruise tracks sampled both the eastern edge of the N gyre and the previously unsampled centre of the N gyre (Fig. 1), allowing the comparison of rates in the two regions.

The aims of this study were (1) to examine the temporal and spatial variability of *P*, *R* and *P*/*R*, and to investigate how this might have affected previous estimates of the metabolic balance of the gyres, (2) to address the idea that contrasting *P*/*R* balances within the N and S gyres arise from characteristic differences in ecosystem functioning and (3) to consider our observations in the context of future global warming.

2. Methods

2.1. Sampling

The six cruises (AMT 12–17) took place between May 2003 and November 2005 on the RRS James Clark Ross (Falkland Island tracks) or the RRS Discovery (South Africa tracks). The northbound cruises (AMT 12, 14 and 16) sampled during boreal spring–summer, embarking from either Port Stanley (Falkland Islands) or Cape Town (South Africa) and disembarking in the UK. The southbound cruises (AMT 13, 15 and 17) started in boreal autumn, departing from the UK and ending in either the Falkland Islands or South Africa. All cruise tracks sampled the centre of the South Atlantic Subtropical Gyre (S gyre, 29 stations) and within the North Atlantic Subtropical Gyre (N gyre, 31 stations). AMT 12, 14, 16 and 17 (June 2003, May 2004, June 2005, October–November 2005) specifically sampled the centre of the N gyre (21°N 35°W, 29°N 37°W, 35°N 43°W, 28°N 39°W) whereas the AMT 13 and 15 cruise tracks (September 2003 and 2004) sampled the east of the N gyre north of the Mauritanian coastal upwelling (Fig. 1).

2.2. Euphotic zone gross production and dark community respiration

Water was collected daily, up to 2 h before dawn, from up to five depths, with a rosette of $24 \times 20\,dm^3$ 'Niskin'-type sampling bottles fitted with a SeaBird 9/11 *plus* CTD system. Gross production (*P*) and dark community respiration (*R*) were determined from *in vitro* changes in dissolved oxygen. Water was collected directly into opaque polypropylene aspirators from depths equivalent to 97% (AMT 14–17 only), 55%, 33%, 14% and 1% of surface irradiance. Irradiance levels were determined from light measurements made the previous day, or by assuming that the deep fluorescence maximum approximated the depth to which 1% of surface irradiance reached (Agusti and Duarte, 1999). The water was siphoned into 125-cm^3 borosilicate glass bottles and 4–5 zero time replicates were fixed within an hour of collection. Two further sets of 4–6 replicates were incubated for

24 h in surface water cooled deck incubators or in temperature controlled water baths at *in situ* temperatures. One set of replicates was incubated in the dark, the other set in the equivalent irradiance to that found at the *in situ* sampling depth. This was controlled using polycarbonate screens incorporating neutral density acrylic of differing transmission (Robinson et al., 2002). Dissolved oxygen concentrations were measured using an automated Winkler titration system with a photometric endpoint (Williams and Jenkinson, 1982). *R* was calculated as the difference between the means of dissolved oxygen concentrations for the zero and the dark replicates, net community production (NCP or *P*−*R*) as the difference between the means for the zero and the light replicates and *P* as the difference between the means for the light and the dark replicates. Due to limitations of sample water volume and analysis time during AMT 12 and 13, we assumed that plankton community structure was homogeneous within the surface 15 m and so incubated a set of replicates sampled from the 55% light depth at 97% of surface irradiance. Flow cytometry data from AMT 13 confirmed that this was a reasonable assumption, since picoplankton cell abundance varied by less than 5% between the two light depths throughout the transect, and nanoplankton varied by 11%. Incubations commenced at dawn (±~1 h), and during hours of darkness the incubators were covered with opaque screens to prevent interference from the ship's deck lights.

Throughout our analysis, we considered rates of *P* and *R* integrated to the base of the euphotic zone (assumed to be the depth of 1% surface irradiance) to facilitate comparisons with recent Atlantic gyre-based studies (Duarte et al., 2001; Serret et al., 2001, 2002; Moran et al., 2004). Integrated rates introduce less bias than volumetric rates, by compensating for imbalances in the water column (Williams, 1998), which is particularly important when comparing rates from different seasons with potentially very different depth profiles (Williams et al., 2004). Rates were integrated (linear trapezoidal integration) from the surface to the 1% light depth (which ranged from 75 to 180 m). Integrations were only performed on volumetric data when the samples' fixing temperatures were within 5 °C of *in situ* temperature, when data were available at more than three depths, and when these data included the surface and 1% light depth (this removed 6% of raw data). The analytical precision on measurements was calculated from the standard error (SE) on a particular set of replicates (calculated as $SD/\sqrt{n}$, where SD is the standard deviation of a set of *n* replicates), and these standard errors were integrated to give errors for the integrated rates. Only volumetric rates that were greater than twice their associated SE were used, although rates at the 1% light depth were often low in comparison to associated errors, so all rates from this depth were included in water column integrations regardless of errors (16% of rates were <2SE). Negative rates of *P* and *R* measured at the 1% light depth were assumed to be zero for the purposes of integration (10% of rates at 1% light depth). Data from the S gyre during AMT 12 include rates with particularly low precision (13 out of 15 volumetric rates <2SE), due to technical limitations. In these cases the median of replicate samples was used rather than the mean, to reduce the influence of extreme values (2% of rates).

The mean of the standard errors on the volumetric rates for all six cruises was 0.15 mmol O_2 m^{-3} day^{-1} for *P* ($n=265$), and 0.13 mmol O_2 m^{-3} day^{-1} for *R* ($n=275$). The mean of the standard errors on the depth integrated rates for all six cruises were 10 mmol O_2 m^{-2} day^{-1} for *P*, and 9 mmol O_2 m^{-2} day^{-1} for *R* ($n=60$ in each case).

The dataset referred to in this study includes 3 days when we were unable to carry out light incubations, so *R* was determined but not *P*. One *P* datapoint had no associated rate of *R* since this rate, measured during a time of technical problems, significantly skewed an otherwise unskewed dataset from normal distribution. The larger dataset (including the four "unpaired" rates) was used throughout, except when paired *t*-tests were used to compare rates of *P* and *R*.

We assumed a PQ of 1 for all carbon/oxygen unit conversions.

2.3. Nitracline and mixed-layer depth

Nitrate concentrations were determined using a Bran+Luebbe AAIII segmented flow colorimetric autoanalyser (Woodward and Rees, 2001). The nitracline (Z_n) was defined as the depth at which nitrate concentrations greater than 0.03 μM were detected. The mixed-layer depth (Z_m) was defined as the depth at which *in situ* temperature changed by more than 0.2 °C m^{-1}. However, in 12 out of 60 cases Z_m could not be determined by this method, and we used the depth at which *in situ* temperature changed by more than 0.1 °C m^{-1}.

2.4. Satellite-derived chlorophyll

Estimates of chlorophyll concentration for six locations on the cruise track were extracted from NASA-supplied sea-viewing wide field-of-view sensor (SeaWiFS) monthly composites. Each sample represents the average chlorophyll during the month over a nominal 9 km × 9 km point. The satellite retrievals use the current operational band switching algorithm, OC4v4 (O'Reilly et al., 1998).

2.5. Gyre boundaries

Sea surface (~7 m) salinity and density were measured underway throughout the cruises using an FSI thermosalinograph. Calibration samples for the salinity measurements were taken daily and analysed using an Autosal 8400B salinometer. Surface chlorophyll concentrations were measured using a Chelsea MKIII Aquatracka fluorometer on the CTD. The fluorometer was calibrated by filtration of 250–500 cm^3 of seawater (Whatman GF/F glassfibre filters; nominal pore size 0.7 μm), extraction in 10 cm^3 90% acetone (HPLC grade) for 18–20 h (dark, 4 °C) and measurement of chlorophyll fluorescence with a TD-700 (Turner Designs) fluorometer (after Welschmeyer, 1994) calibrated with pure Chl *a* standards (Sigma, UK).

The gyre boundaries were determined as far as possible from the position of coincident salinity and density fronts (evident as abrupt changes in the magnitude of the second derivative of salinity and density when plotted against latitude). When the physical changes were not abrupt enough to show a sharp boundary, we used salinity and density data from previous cruises at similar times of year to determine where 'borderline' stations might occur. We then used real-time surface chlorophyll concentrations to determine whether they were indeed gyre stations. Data were not included in the gyre dataset when surface chlorophyll was more than 0.05 mg m^{-3} higher than the chlorophyll concentration measured at the closest station within the gyre, or where surface chlorophyll exceeded 0.2 mg m^{-3}. Due to the different cruise tracks, the latitudinal range of the gyre data was specific to each cruise. The northern extent of the N gyre data lay between 35 and 40°N (depending on the cruise) and the southern extent between 14° and 20°N, except on AMT 13 and 15 when the gyre boundary was crossed at 26–30°N. The northern extreme of the S gyre lay between 10° and 14°S and the southern extreme between 35° and 38°S on AMT 12–15 and between 23° and 27°S on AMT 16 and 17.

2.6. Statistical analysis

The significance of the hypothesis that rates of *P* differed from associated rates of *R* was tested using the paired *t*-test for *P* versus

Table 1a
Euphotic-zone integrated rates of P and R (mmol O_2 m^{-2} d^{-1}) from the N and S gyres.

	Range	Mean (±SD)	Mean spr	Mean aut
AMT 12–17				
N gyre				
P	20–119	63±23	65	59
R	35–133	69±22	68	74
P/R	0.6–1.4	0.9±0.2	1.0	0.8
P vs R		**	n/s	**
S gyre				
P	15–107	58±26	72	42
R	23–149	62±24	67	56
P/R	0.3–1.8	1.0±0.4	1.2	0.7
P vs R		n/s	n/s	**
Combined dataset				
N gyre				
P	10–201	69±41	84	56
R	35–209	98±50	99	77
P/R	0.1–2.1	0.8±0.1	0.9	0.8
P vs R		**	*	**
S gyre				
P	15–107	58±25	68	44
R	7–149	57±24	60	64
P/R	0.3–5.2	1.2±0.2	1.4	0.7
P vs R		n/s	n/s	**

The range and mean (±standard deviation) are shown for rates measured during this study (AMT 12–17) and for those rates in the combined dataset (AMT12–17 plus data at www.amt-uk.org/data/respiration.xls). Also shown are mean rates for spring (spr) and autumn (aut) (April–June and September–November in respective gyres). The significances for the difference between simultaneously measured rates of P and R within each dataset (paired t-tests) are also given. Significance is denoted as ** for $p<0.01$ and * for $p<0.1$. Non-significance is denoted as n/s.

Table 1b
Comparisons of P and R between seasons and gyres using one-way analysis of variance (ANOVA).

Variables tested using ANOVA	Significant difference	ANOVA results	
AMT 12–17			
P between gyres (all seasons)	No	$F_{1,59}=0.91$	$p=0.343$
R between gyres (all seasons)	No	$F_{1,60}=3.30$	$p=0.075$
P between seasons (both gyres)	Yes	$F_{1,59}=9.67$	$p=0.003$
R between seasons (both gyres)	No	$F_{1,60}=0.60$	$p=0.441$
N gyre only			
P between seasons	No	$F_{1,29}=0.30$	$p=0.591$
R between seasons	No	$F_{1,30}=0.31$	$p=0.583$
S Gyre only			
P between seasons	Yes	$F_{1,29}=16.43$	$p=0.000$
R between seasons	No	$F_{1,60}=1.70$	$p=0.203$
Combined dataset			
P between gyres (all seasons)	No	$F_{1,94}=0.89$	$p=0.348$
R between gyres (all seasons)	Yes	$F_{1,96}=22.84$	$p=0.000$
P between seasons (both gyres)	Yes	$F_{1,94}=8.89$	$p=0.004$
R between seasons (both gyres)	Yes	$F_{1,96}=4.11$	$p=0.046$
N gyre only			
P between seasons	No	$F_{1,60}=1.68$	$p=0.199$
R between seasons	Yes	$F_{1,62}=5.36$	$p=0.024$
S gyre only			
P between seasons	Yes	$F_{1,33}=15.13$	$p=0.000$
R between seasons	No	$F_{1,33}=0.01$	$p=0.910$

The results are reported as $F_{a,b}=x$, $p=y$, where F is the mean square to mean square error ratio, the subscripts denote the degrees of freedom and p is the ANOVA critical significance value.

R (Table 1a). For the comparison of datasets with each other (for example, rates measured within a particular gyre between seasons or comparing rates measured in the two gyres), Kolmogrov–Smirnov tests were used to check the normality of datasets, and they were consequently log transformed. One-way analysis of variance (ANOVA) was used to test whether there were significant differences between data measured in the two gyres and between seasons. The results are given in Table 1b.

2.7. Combined dataset of Atlantic P/R measurements

The scope of our P/R dataset was expanded using previously measured rates of P and R that fell within the geographical range of our AMT 12–17 dataset (from the global database at www.amt-uk.org/data/respiration.xls; Robinson and Williams, 2005). This "combined dataset" is specific to the gyre region sampled during AMT 12–17 to ensure spatial comparability between the two datasets. The combined dataset includes data collected between 18° and 38°N, but not stations sampled east of 19°W, or between 19° and 24°W south of 24°N (to avoid stations within the NW African upwelling).

3. Results

3.1. Sampling times in relation to season

Spring sampling times in the N gyre were relatively late in the season, ranging from 19 May (~8 weeks after the vernal equinox) to 21 June (summer equinox). Spring sampling in the S gyre occurred comparatively early in the season, ranging from 3 October (~1 week after the vernal equinox) to 18 November (~1 month before the summer solstice). Boreal autumn sampling was relatively early in the season (19 September–4 November) compared to austral autumn sampling (5 May–3 June, ~2–6 weeks before the start of winter).

3.2. Vertical mixing and nutrient stress

Spring sampling in the S gyre generally coincided with periods of deep mixing (>100 m), in contrast to autumn sampling, when the mixed layer was usually shallower, and defined by a pronounced thermocline. The nitracline in the S gyre was deeper than 100 m at 27 of the 28 stations. However, mixing depths in the N gyre exhibited much less seasonality and all had some degree of stratification, although this was generally weaker in spring than autumn. The nitracline lay below 100 m at 26 of the 30 stations.

Sampling stations were classified according to "nutrient stress", defined after González et al. (2002) from the relative depths of the nitracline (Z_n) and mixed-layer depth (Z_m). Stations where the nitracline lay within the mixed layer were assumed to be under low nutrient stress, whereas those stations with a nitracline lying below the mixed layer ($Z_n-Z_m>0$), were defined as under high nutrient stress.

Therefore in the S gyre, nutrient stress was driven by seasonal changes in water-column stability. Fewer stations were defined as being under high nutrient stress in the S gyre during the spring (when the nitracline lay within the deep mixed layer at 8 of the 16 stations) than in autumn (when the nitracline lay below the thermocline at all 12 stations). In the N gyre, 28 of the 30 stations

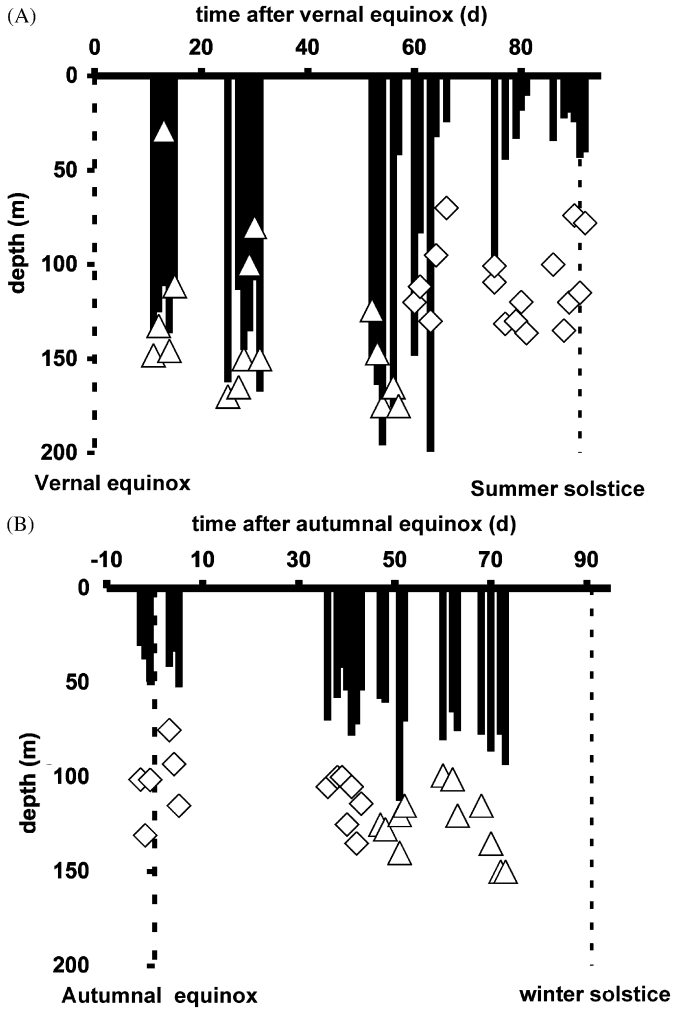

Fig. 2. (A) Spring sampling during AMT 12–17, in relation to the vernal equinox (denoted by the *y*-axis) and the summer solstice (denoted by a dashed vertical line), both ± 1 day depending on the year. Displayed for each sample point is the mixed-layer depth (solid vertical line) and nitracline depth (open diamonds for the N gyre; open triangles for the S gyre). (B) Autumn sampling during AMT 12–17, in relation to the autumnal equinox (denoted by the *y*-axis) and the winter solstice (denoted by a dashed vertical line), both ± 1 day depending on the year. Displayed for each sample point is the mixed-layer depth (solid vertical line) and nitracline depth (open diamonds for the N gyre; open triangles for the S gyre).

were defined as under high nutrient stress, with the nitracline lying below the mixed layer. Fig. 2A shows the mixed layer and nitracline depths of stations sampled in the N and S gyres indicating the relatively higher nutrient stress in the N gyre than in the S gyre during spring. The equivalent data from autumn is shown in Fig. 2B.

3.3. Balance between P and R

The mean, range, and variability of *P* and *R* were similar in both gyres, but the mean rates of *R* were slightly higher than the mean rates of *P* within each gyre (Table 1a). Several Atlantic Ocean studies have derived empirical relationships between *P* and *R* or between *P*/*R* and *P* from which "threshold values" of *P* (below which the system is net heterotrophic) could be calculated (e.g. Gonzalez et al., 2001; Duarte et al., 2001; Serret et al., 2001, 2002; Aristegui and Harrison, 2002). The simplicity of this relationship has been challenged (Serret et al., 2002), and it is unlikely that the relationship is the same between even similarly unproductive systems (Serret et al., 2006). However, the value has been used to extrapolate datasets to longer and larger temporal and spatial scales, so it is relevant to determine how our values compare with previous estimates. The threshold values of *P* for the N and S gyre were 74 and 58 mmol O_2 m^{-2} d^{-1}, respectively (Fig. 3A). Fig. 4 shows integrated rates for the two gyres during AMT cruises 12–17, and there is an apparent seasonal split in the rates of *P* within the S gyre, with autumn and spring rates tending to lie either side of the threshold value.

Considering all data regardless of sampling season, the N gyre was net heterotrophic, and the S gyre was balanced. Rates of *R* were higher than simultaneously measured *P* at 21 out of 30 stations in the N gyre, a statistically significant difference (Table 1a). In the S gyre, *R* exceeds *P* at 17 of the 29 stations but there was no significant difference between the rates of *P* and *R* (Table 1a).

3.3.1. Seasonal variability of P and R

The metabolic balance of the gyres changed with sampling season, and there was significant seasonal variability of *P* within the S gyre (Table 1b). Both gyres were heterotrophic in autumn, but *P*/*R* was higher for both gyres during spring (Table 1a). This change in the *P*/*R* balance was most pronounced within the S gyre, where *P*/*R* was <1 in autumn and >1 during spring, a change apparently driven by variability of *P*. Mean *P* in spring was 70% higher than the autumn mean, a statistically significant seasonal change (Table 1b), but *R* changed much less between seasons. In contrast to the S gyre, there was no significant seasonality of *P* in the N gyre (Table 1b), and *P*/*R* was less than or equal to 1 during both seasons (Table 1a).

4. Discussion

4.1. AMT 12–17 dataset

4.1.1. Balance between P and R

Our results imply that the N gyre is net heterotrophic, and that it is more heterotrophic than the S gyre. This agrees with the persistent net heterotrophy observed in the NAST-E (e.g., Duarte et al., 2001; Serret et al., 2002; Moran et al., 2004) and the contrasting balances (of a net heterotrophic N gyre and more balanced S gyre) measured during the AMT 11 transect in September 2000 (Serret et al., 2002). The threshold values for this study (74 and 58 mmol O_2 m^{-2} d^{-1} for the N and S gyres, respectively) lie within the range of previously published values (summarised in Lopez-Urrutia et al., 2006), but are low compared to previous estimates that are based on O_2-derived *P*/*R* data from the Atlantic: 100 mmol O_2 m^{-2} d^{-1} (N and S Atlantic, Serret et al., 2001) and 92 mmol O_2 m^{-2} d^{-1} (NE subtropical Atlantic, Duarte et al., 2001). It is possible that the contrast between our results and those from the earlier studies arises from differences in temporal/spatial coverage of the datasets. The threshold value of Serret et al. (2001), for example, is based on rates measured at similar times of year to our study, but it includes rates from both productive and oligotrophic open-ocean regions, whereas our value is based only on rates measured within the oligotrophic gyres. The study of Duarte et al. (2001), while confined to the subtropical Atlantic, included rates measured in the Eastern (Canary) coastal province (CNRY, Longhurst, 1998), as far east as 31°N 10.4°W, whereas our N gyre threshold value is based only on data collected west of 20°W, the eastern boundary of the AMT 12–17 cruise tracks. The threshold value derived by Duarte et al. (2001) is also based on measurements from summer and early spring, in contrast to our value, which is derived from measurements made in spring and autumn. Our study included rates

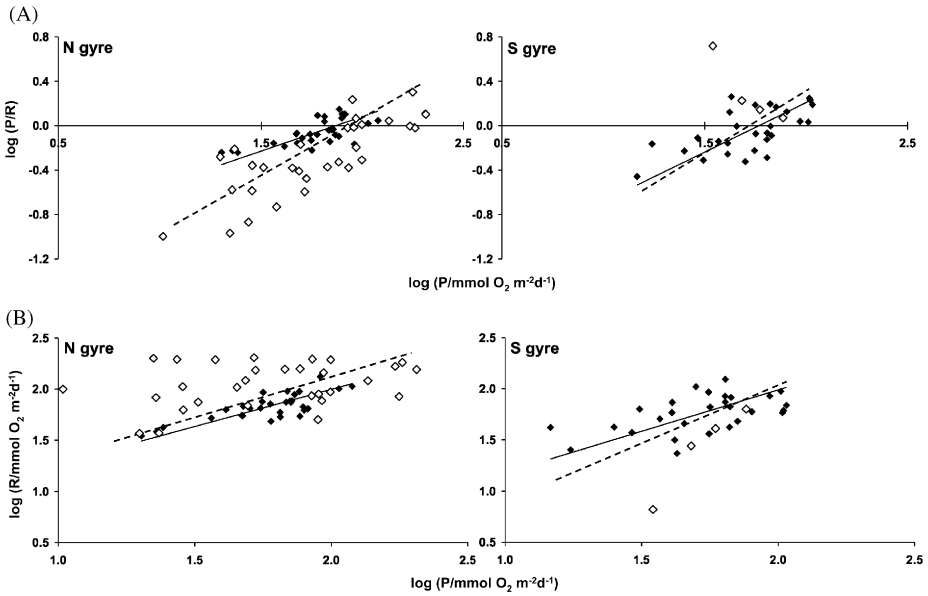

Fig. 3. (A) Relationship between P/R and P in the gyres for AMT 12–17 (closed diamonds) and the measurements from www.amt-uk.org/data/respiration.xls (open diamonds). Model II linear regressions are shown as a solid line for the AMT 12–17 dataset and a dashed line for the combined AMT 12–17 plus www.amt-uk.org/data/respiration.xls dataset with equations as follows: N gyre AMT 12–17: $P/R = 0.07P^{0.62}$, $r = 0.69$, $n = 30$; N gyre AMT 12–17 plus dataset: $P/R = 0.01P^{1.04}$, $r = 0.70$, $n = 61$; S gyre AMT 12–17: $P/R = 0.03P^{0.89}$, $r = 0.64$, $n = 28$; S gyre AMT 12–17 plus dataset: $P/R = 79.4P^{1.10}$, $r = 0.42$, $n = 32$. (B) Relationship between R and P in the gyres for AMT 12–17 (closed diamonds) and the dataset measurements from www.amt-uk.org/data/respiration.xls (open diamonds). Model II linear regressions are shown as a solid line for the AMT 12–17 data and a dashed line for the combined AMT 12–17 plus www.amt-uk.org/data/respiration.xls dataset with equations as follows: N gyre AMT 12–17: $R = 3.47P^{0.73}$, $r = 0.78$, $n = 30$; N gyre AMT 12–17 plus dataset: $R = 3.39P^{0.79}$, $r = 0.34$, $n = 61$; S gyre AMT 12–17: $R = 2.29P^{0.81}$, $r = 0.53$, $n = 28$; S gyre AMT 12–17 plus dataset: $R = 0.59P^{1.14}$, $r = 0.47$, $n = 32$.

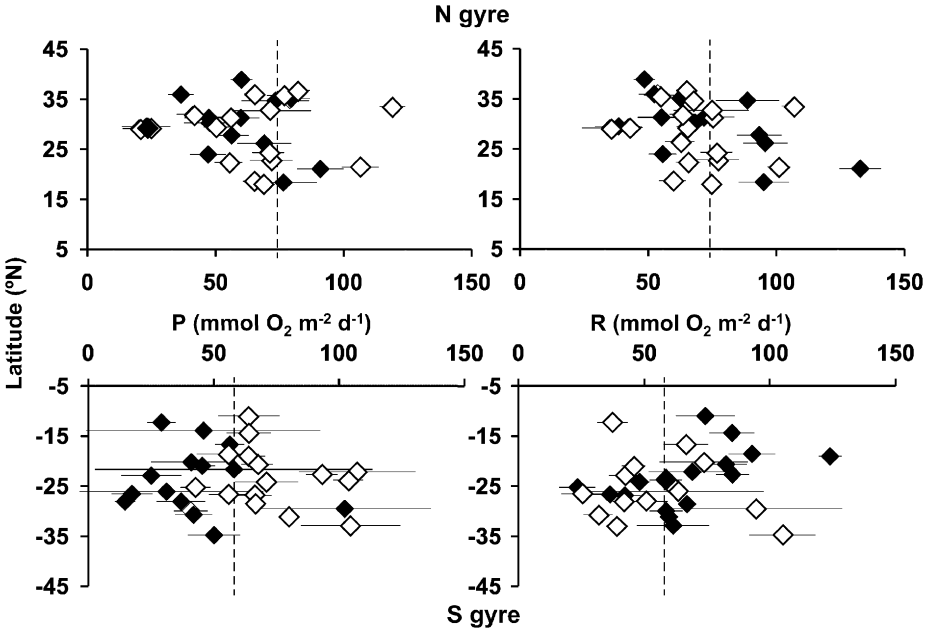

Fig. 4. Rates measured during AMT 12–17. Autumn rates (closed diamonds) and spring rates (open diamonds) are plotted with error bars ±1 SE. Errors were particularly high in the S gyre during AMT 12 due to technical difficulties, but the data is normally distributed and within the range of the other measurements. The dotted vertical line denotes the threshold value of P for each gyre for the AMT 12–17 cruises, and this is also shown on the R plots.

measured beyond the western limits of both the earlier studies (west of 32°W), and rates measured further south than the extent of the previous sampling (as far south as 18°N). Rates of P higher than 100 mmol O_2 m^{-2} d^{-1} (i.e. above the Serret et al. (2002) threshold value) were measured at only 4 of the 30 N gyre stations from our study, and the mean rate of R for the remaining, less productive stations was 61 mmol O_2 m^{-2} d^{-1}, which is only ~50% of the mean rates for similarly unproductive stations in the two earlier studies. This indicates that, even for similarly unproductive waters, rates of respiration were higher during the earlier studies than during AMT 12–17. However, despite, our N gyre threshold value being lower than previous estimates for the region, it is still higher than the mean rate of carbon production estimated for the NAST-E from satellite measurements (~50 mmol O_2 m^{-2} d^{-1}, Duarte et al., 2001), implying that, as suggested by earlier studies, this region cannot be sustained by locally produced carbon alone.

We aim to establish when and where the gyres are most imbalanced in order to help to determine how the observed heterotrophy might be sustained.

4.1.2. Seasonal variability of P and R

The results outlined in the previous section imply that the N gyre is more heterotrophic than the S gyre, but spring sampling in the N gyre occurred relatively late in the season compared to the S gyre, and this may have affected the outcome of our comparison. The surface waters of the gyres are nutrient deplete for the majority of the year, and are separated from the nitracline by well-developed thermoclines; nutrient-limited blooms occurring when stratification breaks down (Longhurst, 1998). However, recent seasonal studies show that primary production within the N gyre peaks during the winter months (Teira et al., 2005), when the mixed layer deepens to the nitracline (Neuer et al., 2002), and SeaWiFS-derived surface chlorophyll concentrations also peak at this time of year (Fig. 5). Seasonality within the S gyre is less well constrained, but we would expect the N gyre to be more productive than the S gyre, and subject to greater seasonal forcing (Longhurst, 1998), consistent with the less-defined seasonal peak for the intra-annual Chl cycle (Fig. 5). However, rates of P measured during our study had similar ranges and means in both gyres, and seasonality of P and P/R were most pronounced in the S gyre. This suggests that our spring sampling in the N gyre, but not in the S gyre, occurred well after rates of P had peaked. This is consistent with the deeper mixing and lower nutrient stress in the S gyre compared to the N gyre, and with the timing of the cruises in relation to the seasonal Chl cycles (Fig. 5). Accordingly, the more marked seasonality in the S gyre does not arise from higher rates of P relative to the N gyre. P in the S gyre was significantly lower during autumn than during spring (Table 1a), and autumn P was lower here than in the N gyre during the same season (Table 1a), which suggests that sampling during our study missed the most productive period for the N gyre.

The more pronounced seasonality of P and P/R within the S gyre was related to the changes in the relative depths of the thermocline and nitracline. The greater degree of heterotrophy measured in the N gyre compared to the S gyre may therefore be a consequence of the more advanced stratification in the N gyre at the time of sampling, notwithstanding the caveat that the most productive season in the N gyre was not sampled. We cannot disregard the possibility that the heterotrophy that was measured in the N gyre is balanced during more autotrophic periods, as observed in temperate ecosystems (Blight et al., 1995; Serret et al., 1999).

4.1.3. Spatial variability in the N gyre

Rates of P and R measured during AMT 12–17 imply that the N gyre is less heterotrophic than estimated by previous studies (Duarte et al., 2001; Serret et al., 2002). This may be a consequence of differences in the spatial coverage of our dataset, compared to earlier studies. Our study included rates measured beyond the southern extreme of previous gyre measurements (between 18° and 25°N), and we measured further west into the gyre than previous studies. However, excluding the data from 18° to 25°N decreased the degree of heterotrophy and the threshold value even more, indicating that rates measured in this region do not account for the differences. Similarly there was no significant difference between P and R measured in the east and west of the N gyre.

4.2. Combined dataset of P and R measurements

The S gyre rate measurements added to our dataset from www.amt-uk.org/data/respiration.xls (Robinson and Williams, 2005) were all from a single AMT cruise (AMT 11, Serret et al., 2002), and the addition of these data to our S gyre dataset ($n = 4$) had no significant effect on the overall range, mean or standard deviation of the rates. The only other published S gyre rates of P and R that we are aware of were collected during AMT 4 and AMT 5; however, sampling was generally outside our gyre boundaries (González et al., 2002). The single rate of P/R that was measured within our study region was not considered in our analysis, since R at this station was 10 times higher than other open-ocean measurements in the database (discussed previously in Serret et al., 2006).

Many more P/R measurements have been made in the N Atlantic than the S Atlantic, and 28 previously published rates could be added to those collected here. This combined N gyre dataset had a much greater range and variability of both P and R, almost double that for the AMT 12–17 data alone (Table 1a). The mean R for the 28 previously published rates was more than 80% higher than the mean R for the AMT 12–17 data (125 mmol O_2 m^{-2} d^{-1} compared with 69 mmol O_2 m^{-2} d^{-1}), although the mean P was similar in both datasets. It is possible that this difference arises from inter-annual variability, since the majority of these higher rates of respiration were measured prior to our study. However, they were also measured at a different time of year to our studies (April and August), and are confined to the northeastern region of the N gyre, so we cannot separate these spatial and temporal influences. We can find no methodological variations between the studies that might account for such pronounced differences in rates.

4.2.1. Balance between P and R

The combined dataset yielded similar results to the AMT 12–17 dataset for the overall balance of P and R in the gyres, but the contrast between the S gyre and N gyre was much more

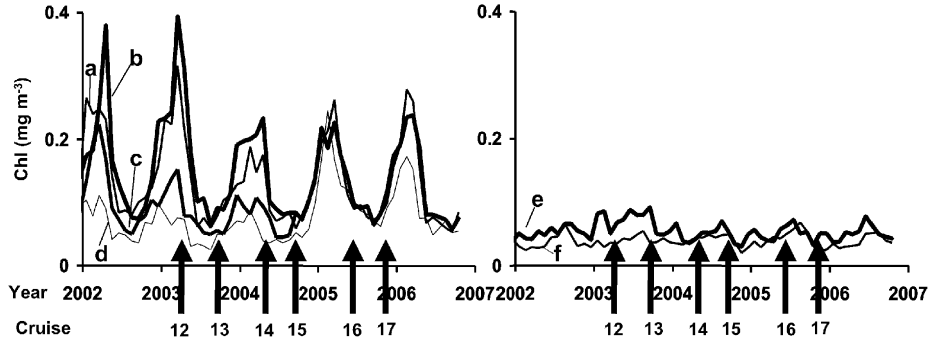

Fig. 5. SeaWiFS monthly mean surface chlorophyll concentrations for January 2002–December 2006 at (a) 35°N 23°W, (b) 36°N 20°W, (c) 30°N 21°W, (d) 29°N 37°W, (e) 26°S 25°W, (f) 19°S 27°W. The arrows denote the approximate timings of the cruises.

pronounced. Comparing P at each station with associated rates of R, the N gyre was significantly heterotrophic but the S gyre was balanced (Table 1a), reflected in the means of P/R, which were 0.8 and 1.2 in the N and S gyre respectively. The difference between the "threshold values" for the two gyres also increased, with the N gyre threshold value increasing to 85 mmol O_2 m^{-2} d^{-1}, but the S gyre value decreasing to 55 mmol O_2 m^{-2} d^{-1}. The increased imbalance in the N gyre was driven by the higher rates of R measured in previous studies compared to those measured during AMT 12–17 (Fig. 3B), and the shift in P/R is immediately apparent from the regression of P/R and P (Fig. 3A). However, the contrast between the balances in the two gyres also increased due to the addition of previously published data to our S gyre dataset, which increased the overall P/R balance (Fig. 3A).

4.2.2. Seasonal variability of P and R

The seasonality of the P/R balance observed during AMT 12–17 was also evident within the combined dataset. Both gyres were most heterotrophic in autumn, when rates of R were higher than associated rates of P (Table 1a). In spring the S gyre was balanced, but the N gyre was heterotrophic (Table 1a). Previously published spring rates from the S gyre that were added to the AMT 12–17 dataset were all autotrophic. They were measured early in the season (2–5 October 2000) and were associated with deep mixing (132–172 m) to the nitracline, as for the majority of spring rates measured within the S gyre during AMT 12–17. Within the combined dataset, the "high nutrient stress" stations were more heterotrophic than the "low nutrient stress" stations. Mean P/R for the high and low stress groups were 0.9 and 1.6, respectively (t-test, $p<0.1$), and P was lower in the high stress group than in the low stress group (54 and 65 mmol O_2 m^{-2} d^{-1}, respectively, unpaired t-test, $p<0.1$). The relationship between P/R and "nutrient stress" is shown in Fig. 6. In the N gyre, 26 of the 29 stations had $Z_n-Z_m<0$, and 20 of these were heterotrophic. However, those stations with nitraclines lying below a pronounced thermocline ($n=11$) were all heterotrophic.

The N gyre combined dataset included rates from April to August, months that were not sampled during AMT 12–17. Mean P for April was higher than for any other month covered by the study (116 mmol O_2 m^{-2} d^{-1}), and rates reached 204 mmol O_2 m^{-2} d^{-1}, the maximum rate in the combined dataset, whereas in August 1998, the N gyre was extremely heterotrophic (González et al., 2002). Mean P for August (34 mmol O_2 m^{-2} d^{-1}) was lower, and mean R was higher (153 mmol O_2 m^{-2} d^{-1}), than the mean rate for any other month included in this study (Fig. 7). The measurements from these months come from a single set of cruises (González et al., 2002), but we can find no variation in our methodology that would give rise to such pronounced differences. The variability in P agrees with that observed for PP in the NAST-E (Teira et al., 2005), with mean PP during summer being about half the magnitude of the mean for spring and autumn.

Our analysis also implies that the N gyre is more heterotrophic than the S gyre, but that this contrast is at least exacerbated, if not caused, by the timing of our measurements. The S gyre dataset was biased towards spring periods of deep mixing, whereas the N gyre dataset spans April–November, missing the most productive months. The most autotrophic data from our combined N gyre dataset come from April, but the most autotrophic period in the N gyre is likely to be the winter months (e.g. December–April, Fig. 5; November–March, Fig. 7) and these were not covered by the database. Linear interpolation of all our N gyre rates, measured over a 7-month period, gives rise to a carbon deficit of 36 mmol C m^{-2} d^{-1} (7533 mmol C m^{-2} over 208 days, assuming a PQ of 1), which, although slightly higher than a straightforward average of P minus R at each station, is lower than the deficit of 53 mmol C m^{-2} d^{-1} calculated from previous measurements within the N gyre (Robinson and Williams, 2005; Duarte et al., 2001; Serret et al., 2002). To support this deficit by microbial production alone over the remaining 5 months would require a net carbon production of 48 mmol C m^{-2} d^{-1} during this period (7533 mmol C m^{-2} over 157 days). Mean NCP during March 2001 in the frontal zone of the N gyre (41.5–44.5N) was 62.5 mmol O_2 m^{-2} d^{-1}, and mean P was 108 mmol O_2 m^{-2} d^{-1} (Maixandeau et al., 2005). Assuming a similar degree of seasonality in P as observed for PP (winter rates a factor of ~6 higher than summer rates, Teira et al., 2005) this is potentially only ~50% of P at the most productive time. Of course, the actual ratio between summer and winter P is unlikely to be as high as the seasonal ratio for PP, since PP becomes increasingly comparable to NCP as productivity decreases (Marra and Barber, 2004). Nevertheless, it suggests that 108 mmol O_2 m^{-2} d^{-1} is unlikely to be a production maximum for the year, and that the gyre is likely to be more autotrophic earlier

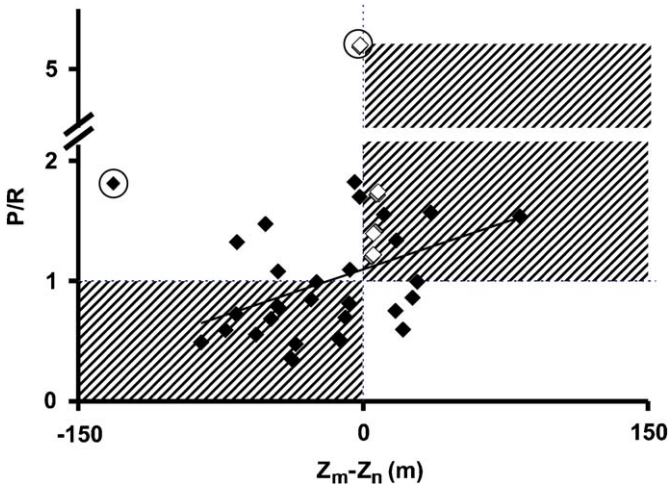

Fig. 6. Relationship between P/R and nutrient stress at stations within the S gyre during AMT 12–17 (closed diamonds) and AMT 11 (open diamonds). Z_m is the mixed-layer depth and Z_n the nitracline depth. When Z_m-Z_n is positive, stations are defined as having low nutrient stress and when Z_m-Z_n is negative, stations are defined as being under high nutrient stress. The equation of the regression line shown, which excludes the circled points, is $y=0.0052x+1.0968$, $r^2=0.21$, $n=30$, $p(x)<0.05$. Areas where high nutrient stress coincides with $P/R<1$ and where low nutrient stress coincides with $P/R>1$ are shaded.

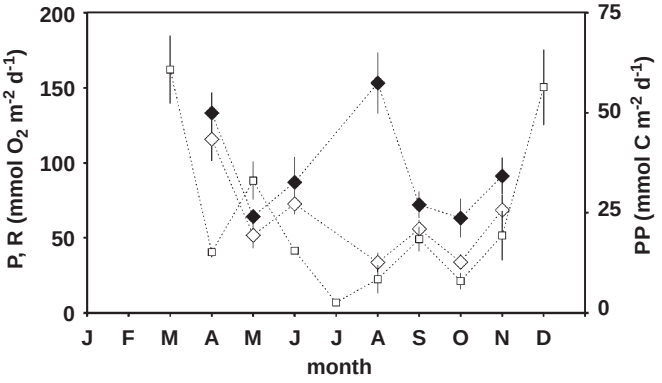

Fig. 7. Monthly means of P (open diamonds) and R (closed diamonds) in the N gyre measured between August 1998 and November 2005 (www.amt-uk.org/data/respiration.xls). Also shown are the monthly means of primary production (PP) for the NAST-E (open squares) taken from Teira et al. (2005). Error bars are the standard error for each month.

in the season, closer to the winter peak in production. Our analysis implies that heterotrophy measured during less productive months could be supported by carbon accumulated during more productive seasons.

The conclusions of our analysis, that the contrast in P/R between the two gyres is partly related to water-column stability at the time of sampling, is particularly important in the context of the suggestion that climate warming will lead to increased stratification and lower productivity within the gyres (Sarmiento et al., 2004). The thermoclines within the gyres are deepening, the gyre extent is increasing (McClain et al., 2004), and decadal changes in N Atlantic carbon cycling have been related to reductions in nutrient availability, induced by increases in sea surface temperatures (Gruber et al., 2002; Gregg et al., 2003; Behrenfeld et al., 2006). If, as our analysis suggests, net heterotrophy in the gyres will increase with increased nutrient stress, then studies such as AMT, which repeatedly sample the same region at the same time of year, are extremely important, because they will help to identify long-term trends (Karl et al., 2001). This tendency of decreasing P/R with increasing nutrient stress is in addition to the tendency for decreasing P/R with increasing temperature as estimated by Lopez-Urrutia et al. (2006).

As the balance between P and R does not only depend on local P (Serret et al., 2006), it is important that the sources of carbon to the region are quantified as well as any predicted change in their magnitude due to environmental change.

4.2.3. Spatial variability in the N gyre

We examined the spatial variability of P and R in the N gyre by performing regression analysis on the mean rates for 3° bins of longitude. Both P and R decreased overall from the gyre edge to the centre, but R decreased more than P (Fig. 8). Throughout this work, no distinction is made between Longhurst's biogeographic NAST-E, NAST-W and NATR (North Atlantic Tropical Gyre) provinces for our analysis. We refer instead to broader, real-time hydrographically defined gyre regions. The majority of the rates in our N gyre dataset lie within either the NAST-E or the NATR, but the three most westerly rates from our dataset fall within the NAST-W province. Longhurst (1998) makes the NAST-E/-W subdivision because the ecology of the eastern and western basins differ, and this is consistent with recent studies which show that phytoplankton growth rates (Marañón, 2005) and export production (Neuer et al., 2002) are significantly different at the outer edges of the two provinces. Excluding the three rates measured in the NAST-W from our dataset does not significantly change the overall estimates of the P/R balance in the N gyre, but when these three rates are excluded from our N gyre dataset, the significance of the regressions show a marked increase, with r^2 increasing (from 0.01 to 0.26 for P and from 0.33 to 0.86 for R) and p decreasing (from 0.15 to 0.03 for P and from <0.001 to <0.0001 for R) (Fig. 8). Excluding those rates measured to the south of the NAST-E province (18–25°N, $n=11$) did not significantly alter the gradient or intercept of the regressions, indicating that our comparatively lower carbon deficit is not caused by the inclusion of these rates. The observed decrease in R from the edge to the centre of the gyre might explain why the gyre was apparently less heterotrophic during AMT 12–17, which spanned 20–45 °W, than during previous studies that were restricted to the northeast of the gyre, and suggests that previous estimates of threshold values and carbon deficits, extrapolated to the NAST-E as a whole, are too high.

Our combined dataset of P and R, comprising rates measured in the N and S gyres between 1998 and 2005, indicates that the N gyre is less heterotrophic than previously estimated (Duarte et al., 2001; Serret et al., 2002), but that it still tends towards net heterotrophy. However, the dataset is still heavily biased towards measurements from the east of the gyre, so to take account of the observed spatial variability within the gyre, we calculated a spatially weighted mean of P–R in the N gyre (from the linear interpolation between the longitude of measurements), which was $\sim$19 mmol O_2 m^{-2} d^{-1}. This is lower than the estimated mean carbon production for the NAST-E (e.g. $\sim$50 mmol C m^{-2} d^{-1}; Duarte et al., 2001), and lower than estimations of dissolved organic carbon (DOC) accumulation in the Azores front region ($\sim$47 mmol C m^{-2} d^{-1}, Doval et al., 2001) suggesting that locally sustained net heterotrophy in the N gyre is more feasible than for previous estimates, and highlighting the need for increased spatial coverage of data within the gyres. Our estimated mean ($\sim$19 mmol O_2 m^{-2} d^{-1}, calculated from integrated rates with an average error of $\sim$10 mmol O_2 m^{-2} d^{-1}) compares better with the basin-scale estimate of net heterotrophy calculated by Hansell et al. (2004) of 2.5 mmol O_2 m^{-2} d^{-1} (calculated assuming a PQ of 1 and the surface area of 10×10^{12} m^2 quoted).

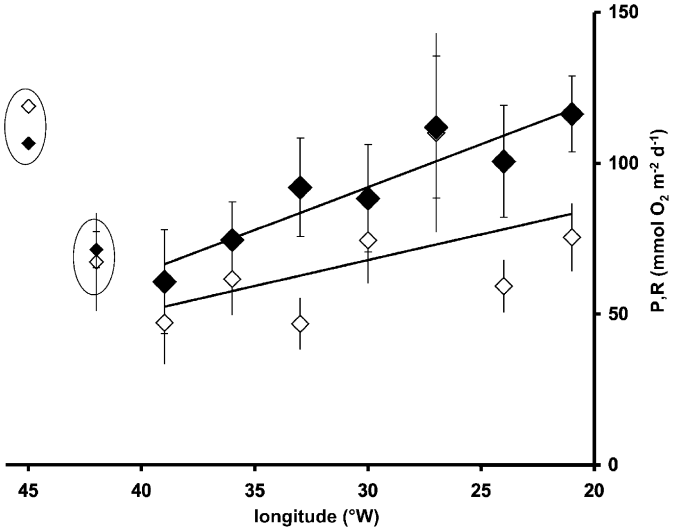

Fig. 8. Mean P (open diamonds) and R (closed diamonds) for 3° bins, centred around the longitude displayed on the x-axis. Regression equations are: $P=-1.7x+119$, $r^2=0.26$, $n=60$, and $R=-2.8x+177$, $r^2=0.86$, $n=62$, where x = bin centre (°W). Circled points are from the NAST-W and not included in the regression equation.

However, the observed gradient in Fig. 8 also could be indicative of an external source of carbon for the N gyre originating, for example, in the northwest African upwelling (Serret et al., 2006) or the atmosphere (Duarte et al., 2006). A recent study suggests that there is a measurable source of atmospheric carbon to the NE Atlantic, and although the magnitude is relatively low compared to our carbon deficit ($\sim$1 mmol C m^{-2} d^{-1}, Duarte et al., 2006), it can significantly affect the P/R balance during high deposition events. The possibility of an external upwelling source has serious implications in the context of a recent study which predicts that global warming is likely to increase the extent of the subtropical gyres, while upwelling systems remain unchanged (Sarmiento et al., 2004). This implies that, in the N gyre, increased heterotrophy related to increased nutrient stress could be exacerbated by a supply of carbon produced outside the gyre.

5. Conclusions

Our data indicate that the N gyre is heterotrophic, and that it is more heterotrophic than the S gyre. However, the P/R balance

changes with season in both gyres, and there is significant temporal variability of *P* in the S gyre, which is related to water-column stability and nutrient availability. We are unable to say whether production between November and April in the N gyre is sufficient to support the heterotrophy measured between April and November without a more seasonally representative dataset. The positive relationship between net heterotrophy and nutrient stress suggests a positive feedback of increasing CO_2 emissions caused by increased stratification predicted in model climate change scenarios. The relationship between *P*/*R* and *P* in the N gyre varied, depending on the temporal and spatial range of the measurements, possibly indicative of an external carbon source originating in the east of the N gyre.

Acknowledgements

This study was supported by the UK Natural Environment Research Council through the Atlantic Meridional Transect consortium (NER/O/S/2001/00680). This is Contribution no. 167 of the AMT programme. We thank Jan Kaiser and Chris Lowe for useful discussions, Gavin Tilstone for statistical advice and Steve Groom (Remote Sensing Data Analysis Service) for assistance with satellite data analysis. We thank the officers and crews of RRS James Clark Ross and Discovery, the principal scientists from AMT 12–17, Alex Poulton and Anna Hickman for calibrating the *in situ* chlorophyll data, and also the AMT team members who helped with the collection, transportation and preparation of water samples during each cruise. SeaWiFS data are courtesy of NASA and Orbimage.

References

Agusti, S., Duarte, C.M., 1999. Phytoplankton chlorophyll *a* distribution and water column stability in the central Atlantic Ocean. Oceanologica Acta 22 (2), 193–203.

Aristegui, J., Harrison, W.G., 2002. Decoupling of primary production and community respiration in the ocean: implications for regional carbon studies. Aquatic Microbial Ecology 29, 199–209.

Behrenfeld, M.J., O'Malley, R.T., Siegel, D.A., McClain, C.R., Sarmiento, J.L., Feldman, G.C., Milligan, A.J., Falkowski, P.G., Letelier, R.M., Boss, E.S., 2006. Climate-driven trends in contemporary ocean productivity. Nature 444, 752–755.

Blight, S.P., Bentley, T.L., Lefevre, D., Robinson, C., Rodrigues, R., Rowlands, J., Williams, P.J.leB., 1995. Phasing of autotrophic and heterotrophic plankton metabolism in a temperate coastal ecosystem. Marine Ecology Progress Series 128, 61–75.

Doval, M.D., Alvarez-Salgado, X.A., Perez, F.F., 2001. Organic matter distributions in the eastern North Atlantic-Azores front region. Journal of Marine Systems 30, 33–49.

Duarte, C.M., Agusti, S., Aristegui, J., González, N., Anadón, R., 2001. Evidence for a heterotrophic subtropical northeast Atlantic. Limnology and Oceanography 46 (2), 425–428.

Duarte, C.M., Dachs, J., Llabres, M., Alonso-Laita, P., Gasol, J.M., Tovar-Sánchez, A., Sañudo-Wilhemy, S., Agustí, S., 2006. Aerosol inputs enhance new production in the subtropical northeast Atlantic. Journal of Geophysical Research 3.

Emerson, S., Quay, P., Karl, D., Winn, C., Tupas, L., Landry, M., 1997. Experimental determination of the organic carbon flux from open-ocean surface waters. Nature 389 (6654), 951–954.

Gonzalez, N., Anadon, R., Mourino, B., Fernandez, E., Sinha, B., Escanez, J., de Armas, D., 2001. The metabolic balance of the planktonic community in the North Atlantic Subtropical Gyre: the role of mesoscale instabilities. Limnology and Oceanography 46 (4), 946–952.

González, N., Anadón, R., Marañón, E., 2002. Large-scale variability of planktonic net community metabolism in the Atlantic Ocean: importance of temporal changes in oligotrophic subtropical waters. Marine Ecology Progress Series 233, 21–30.

Gregg, W.W., Conkright, M.E., Ginoux, P., O'Reilly, J.E., Casey, N.W., 2003. Ocean primary production and climate: global decadal changes. Geophysical Research Letters 30 (15) (Art. no. 1809).

Gruber, N., Keeling, C.D., Bates, N.R., 2002. Interannual variability in the North Atlantic Ocean carbon sink. Science 298 (5602), 2374–2378.

Hansell, D.A., Ducklow, H.W., Macdonald, A.M., Baringer, M.O.N., 2004. Metabolic poise in the North Atlantic Ocean diagnosed from organic matter transports. Limnology and Oceanography 49, 1084–1094.

Karl, D.M., Bidigare, R.R., Letelier, R.M., 2001. Long-term changes in plankton community structure and productivity in the North Pacific Subtropical Gyre: the domain shift hypothesis. Deep-Sea Research II 48 (8–9), 1449–1470.

Longhurst, A., 1998. Ecological Geography of the Sea. Academic Press, San Diego.

Lopez-Urrutia, A., San Martin, E., Harris, R.P., Irigoien, X., 2006. Scaling the metabolic balance of the oceans. Proceedings of the National Academy of Sciences of the United States of America 103 (23), 8739–8744.

Maixandeau, A., Lefevre, D., Fernandez, I.C., Sempere, R., Sohrin, R., Ras, J., Van Wambeke, F., Caniaux, G., Queguiner, B., 2005. Mesoscale and seasonal variability of community production and respiration in the surface waters of the NE Atlantic Ocean. Deep-Sea Research I 52 (9), 1663–1676.

Marañón, E., 2005. Phytoplankton growth rates in the Atlantic subtropical gyres. Limnology and Oceanography 50, 299–310.

Marañón, E., Behrenfeld, M.J., González, N., Mouriño, B., Zubkov, M.V., 2003. High variability of primary production in oligotrophic waters of the Atlantic Ocean: uncoupling from phytoplankton biomass and size structure. Marine Ecology Progress Series 257, 1–11.

Marra, J., Barber, R.T., 2004. Phytoplankton and heterotrophic respiration in the surface layer of the ocean. Geophysical Research Letters 31 (9), L09314.

McClain, C.R., Signorini, S.R., Christian, J.R., 2004. Subtropical gyre variability observed by ocean-color satellites. Deep-Sea Research II 51 (1–3), 281–301.

Moran, X.A.G., Fernández, E., Pérez, V., 2004. Size-fractionated primary production, bacterial production and net community production in subtropical and tropical domains of the oligotrophic NE Atlantic in autumn. Marine Ecology Progress Series 274, 17–29.

Neuer, S., Davenport, R., Freudenthal, T., Wefer, G., Llinas, O., Rueda, M.J., Steinberg, D.K., Karl, D.M., 2002. Differences in the biological carbon pump at three subtropical ocean sites. Geophysical Research Letters 29 (18) (Art. no. 1885).

O'Reilly, J.E., Maritorena, S., Mitchell, B.G., Siegel, D.A., Carder, K.L., Garver, S.A., Kahru, M., McClain, C., 1998. Ocean color chl-a algorithms for SeaWiFS. Journal of Geophysical Research 103, 24937–24953.

Pelegri, J.L., Aristeguí, J., Cana, L., Gonzalez-Davila, M., Hernandez-Guerra, A., Hernandez-Leon, S., Marrero-Diaz, A., Montero, M.F., Sangra, P., Santana-Casiano, M., 2005. Coupling between the open ocean and the coastal upwelling region off northwest Africa: water recirculation and offshore pumping of organic matter. Journal of Marine Systems 54 (1–4), 3–37.

Robinson, C., Williams, P.J.leB., 2005. Respiration and its measurement in surface marine waters. In: del Giorgio, P.A., Williams, P.J.leB. (Eds.), Respiration in Aquatic Ecosystems. Oxford University Press, Oxford, pp. 147–180.

Robinson, C., Serret, P., Tilstone, G., Teira, E., Zubkov, M.V., Rees, A.P., Woodward, E.M.S., 2002. Plankton respiration in the Eastern Atlantic Ocean. Deep-Sea Research I 49 (5), 787–813.

Sarmiento, J.L., Slater, R., Barber, R., Bopp, L., Doney, S.C., Hirst, A.C., Kleypas, J., Matear, R., Mikolajewicz, U., Monfray, P., Soldatov, V., Spall, S.A., Stouffer, R., 2004. Response of ocean ecosystems to climate warming. Global Biogeochemical Cycles 18 (3), GB3003.

Serret, P., Fernandez, E., Sostes, J.A., Anadon, R., 1999. Seasonal compensation of microbial production and respiration in a temperate sea. Marine Ecology Progress Series 187, 43–57.

Serret, P., Robinson, C., Fernández, E., Teira, E., Tilstone, G., 2001. Latitudinal variation of the balance between plankton photosynthesis and respiration in the eastern Atlantic Ocean. Limnology and Oceanography 46 (7), 1642–1652.

Serret, P., Fernández, E., Robinson, C., 2002. Biogeographic differences in the net ecosystem metabolism of the open ocean. Ecology 83 (11), 3225–3234.

Serret, P., Fernández, E., Robinson, C., Woodward, E.M.S., Pérez, V., 2006. Local production does not control the balance between plankton photosynthesis and respiration in the open Atlantic Ocean. Deep-Sea Research II 53 (14–16), 1611–1628.

Teira, E., Mouriño, B., Marañón, E., Pérez, V., Pazo, M.J., Serret, P., de Armas, D., Escanez, J., Woodward, E.M.S., Fernández, E., 2005. Variability of chlorophyll and primary production in the Eastern North Atlantic Subtropical Gyre: potential factors affecting phytoplankton activity. Deep-Sea Research I 52 (4), 569–588.

Welschmeyer, N.A., 1994. Fluorometric analysis of chlorophyll *a* in the presence of chlorophyll *b* and phaeopigments. Limnology and Oceanography 39, 1985–1992.

Williams, P.J.leB., 1998. The balance of plankton respiration and photosynthesis in the open oceans. Nature 394, 55–57.

Williams, P.J.leB., Jenkinson, N.W., 1982. A transportable micro-processor controlled precise Winkler titration suitable for field station and shipboard use. Limnology and Oceanography 27, 576–584.

Williams, P.J.L., Morris, P.J., Karl, D.M., 2004. Net community production and metabolic balance at the oligotrophic ocean site, station ALOHA. Deep-Sea Research I 51 (11), 1563–1578.

Woodward, E.M.S., Rees, A.P., 2001. Nutrient distributions in an anticyclonic eddy in the North East Atlantic Ocean, with reference to nanomolar ammonium concentrations. Deep-Sea Research II 48 (4–5), 775–794.